analytical chemistry

Article

Cite This: *Anal. Chem.* 2019, 91, 12238−12245

pubs.acs.org/ac

Enrichment−Stowage−Cycle Strategy for Ultrasensitive Electrochemiluminescent Detection of HIV-DNA with Wide Dynamic Range

Zhen Wu, Fanwei Luo, Wei Wen,* Xiuhua Zhang, and Shengfu Wang*

Hubei Collaborative Innovation Center for Advanced Organic Chemical Materials, Ministry of Education Key Laboratory for the Synthesis and Application of Organic Functional Molecules and College of Chemistry and Chemical Engineering, Hubei University, Wuhan 430062, P. R. China

Supporting Information

ABSTRACT: Sensitive detection of human immunodeficiency virus DNA (HIV-DNA) is essential for timely diagnosis and cure of the illness. Herein, a novel "enrichment−stowage−cycle" strategy was proposed to fabricate a multiple amplified electrochemiluminecence (ECL) biosensor for HIV-DNA detection. On the basis of the enrichment role of magnetic nanobeads, assembly role of copolymer nanospheres and strand displacement amplification (SDA), the processes were named as "enrichment", "stowage", and "cycle", respectively. The method employed electrochemiluminescent nanospheres (ENs) as signal labels by assembling three layers of CdSe/ZnS quantum dots (QDs) onto the surface of copolymer nanospheres. Compared to QDs, the same concentration of ENs can the enhance the ECL intensity by about 11.3-fold. SDA could further amplify the signals by about 3.77-fold, possessing high sensitivity for low-abundant biomarkers detection. The integration of magnetic separation improved detection specificity and stability, making the method possible for practical application. On the basis of magnetic separation, ENs and SDA, the ECL biosensor realized ultrasensitive detection of 39.81 fM HIV-DNA, which was more sensitive than other HIV-DNA analytical methods, with a wide dynamic range of 0.05 pM to 50 nM. The successful detection of HIV-DNA in complex samples with good sensitivity and accuracy indicated its potential utilization in early judgment of diseases and fabrication of signal amplification platforms.

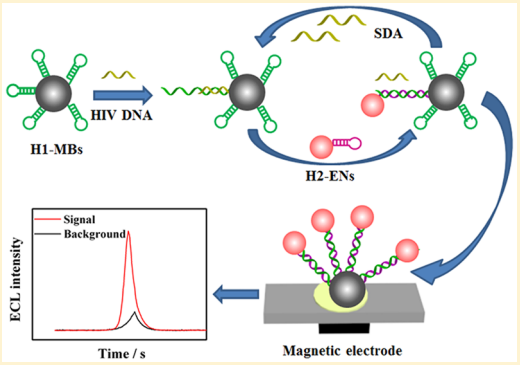

Acquired immune deficiency syndrome (AIDS) was first documented in America in 1981, and outbreak occurred across Asia as the disease spread quickly. AIDS is a serious infectious disease caused by human immunodeficiency virus (HIV) and continues to pose a major threat to human health. HIV can destroy peoples' immunity and lead to a variety of diseases and cancers in the human body, which is one of the most deadly infectious diseases.[1] Since the beginning of the epidemic, more than 70 million people have been infected with HIV, including 35 million deaths.[2] Thus, quantitative detection of HIV is important for the timely diagnosis and cure of AIDS. Traditional strategies have been commonly used for HIV antibody, antigen or DNA detection, including virus neutralization test, serologic tests, enzyme-linked immunosorbent assay,[3] Western blot assay, and polymerase chain reaction.[4,5] Although most of the assays are accurate and reliable, they often suffer from the limitations of insufficient sensitivity, tedious procedures, and time-consumption in the early diagnosis of HIV.[6] Therefore, it is significant to develop sensitive, simple, rapid, and low-cost methods to detect HIV. Until now, many means have been proposed for HIV measurement, such as colorimetric method,[7] electrochemistry,[8,9] fluorescence,[10,11] and surface plasmon resonance (SPR).[12] In addition to such methods, ECL is a better alternative analysis tool due to its high sensitivity, simple optical setup, excellent temporal and spatial controllability, and low background signal without the need of a light source. These unique properties have facilitated ECL a powerful technique for metal ions, small molecules, and biomarker detection, environmental monitoring, as well as food and water testing.[13−16]

Since the first publication on the ECL of Si QDs in 2002,[17] QDs has emerged as a new and popular kind of ECL emitter. Due to its unique properties of size/surface controlled luminescence and wonderful stability without photobleaching problems, the combination of QDs with ECL will enhance sensitivity and make analytical detection a reality. However, this approach is difficult to satisfy the requirements of early detection of low-abundant biomarkers because of the low luminescence quantum efficiency of QDs compared to luminol or $Ru(bpy)_3^{2+}$.[18,19] Some signal amplification strategies based on element doping to improve the luminescence efficiency of emitters, including a carrier technique to increase the loading of signal labels and target recycling amplification strategy, have

Received: April 24, 2019
Accepted: September 5, 2019
Published: September 5, 2019

DOI: 10.1021/acs.analchem.9b01969
Anal. Chem. 2019, 91, 12238−12245

Scheme 1. Illustration of the Multiple Amplified ECL Biosensor for HIV-DNA Detection

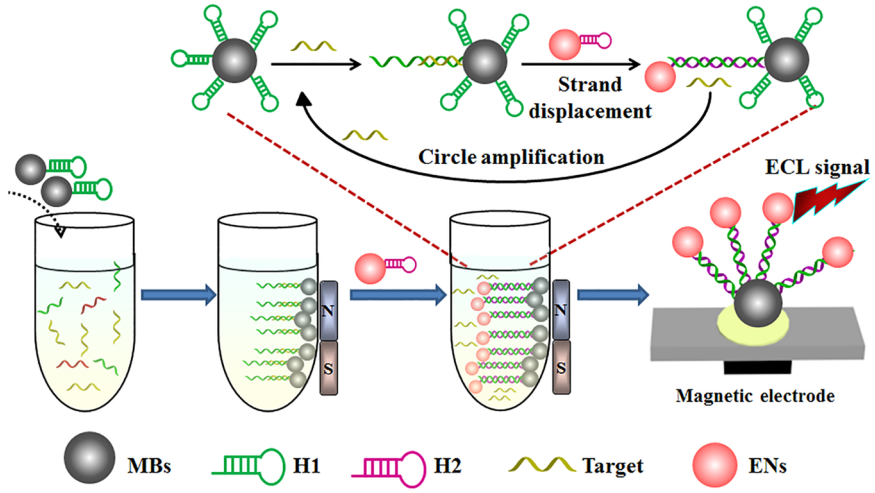

been fabricated to improve the analytical sensitivity.[20−23] For example, N-doped TiO_2 nanotubes were reported to obtain a 10.6-fold ECL signal enhancement.[20] Multiwalled carbon nanotube-modified electrodes improved the ECL signal by 5.3-fold by promoting electron transfer between QDs and electrodes.[21] Target recycling amplification strategy based on exonuclease was reported for as low as 0.12 pM Hg^{2+} detection.[22] Strand displacement amplification (SDA) can recycle the target many times and achieved a detection limit of 0.76 pM toward HIV-DNA.[23] Compared with enzyme-assisted approaches, SDA is a simpler and efficient target enhancement amplification method without any enzyme catalysis or the requirement of strict incubation conditions. However, the limited amplification efficiency and the urgent requirement of high sensitivity for low-abundant biomarker detection facilitated researchers to propose multiple signal amplification. Guo et al. designed a double signal amplification strategy by combination of Au nanoparticles and $Ru(bpy)_3^{2+}$-embedded Si nanospheres (Ru@SNPs).[24] Han et al. further proposed a triply amplified biosensor based on Au-graphene hybrids (Au-GN), Ru@SNPs, and biotin−streptavidin−biotin structure.[25]

Despite sensitivity, detection accuracy is also an important factor to be considered for analytical method. The analysis of nucleic acids in a complex environment usually meets the difficulty of signal accuracy resulted from the interference of plentiful coexisting components.[26] The experimental results may be false positive or false negative signals, which prevent physicians from making an accurate diagnosis and treatment. Thus, samples are usually needed for complicated and time-consuming pretreatment processes to decrease background and coexisting components interference. Several effective technologies have been reported to enrich and separate targets from complex samples, including chromatography, magnetic nanobeads (MBs), and capillary electrophoresis.[27−29] Among them, MBs have been proven to be a powerful separation tool owing to its large specific surface area, rich functional groups, superparamagnetism, and reaction flexibility. Currently, MBs have been widely used in various analytical methods, including electrochemistry,[30,31] fluorescence,[32−34] lateral flow immunoassay,[35] microfluidic chip,[36] and ECL[19,37] sensors. Therefore, it is interesting to combine the idea of MBs and multiple amplification strategies to construct ECL biosensors with high sensitivity and accuracy.

Herein, we proposed an "enrichment−stowage−cycle" strategy to develop a nonenzymatic and multiple amplified ECL biosensor for ultrasensitive detection of HIV-DNA in complex samples. In clinical diagnosis, HIV-DNA detection can be regarded as an important index to reflect the situation of HIV. On the basis of ENs, SDA, and magnetic separation, multiple signal amplification was achieved. As shown in Scheme 1, hairpin DNA functional MBs (H1-MBs) can achieve efficient enrichment and separation of target HIV-DNA from a complex matrix. The use of MBs can save time and simplify operation without sample pretreatment. The addition of another hairpin DNA modified ENs (H2-ENs) could initiate an SDA reaction resulted from the increasing binding sites between H2 and H1. On the basis of SDA, more ENs can be captured on the surface of MBs through cycling reaction, which was beneficial for low-abundant biomarker detection. Finally, the magnetic complexes were captured on a magnetic glassy carbon electrode (M-GCE) surface and strong ECL signals could be obtained in the presence of coreactant $K_2S_2O_8$. ENs were prepared by assembling three layers of QDs on the surface of copolymer nanospheres, which can effectively improve detection sensitivity as signal labels. Using MBs as capture carriers, SDA for signal enhancement, and assembled ENs as signal labels, the developed method behaved with excellent amplification efficiency, good specificity, and high sensitivity.

EXPERIMENTAL SECTION

Reagents and Instruments. Magnetic nanobeads (MBs) (500 nm) with carboxyl groups were supplied by Ademtech SA (Pessac, France). A magnetic glassy carbon electrode (M-GCE) was purchased from Gaoshi Ruilian Technology Co., Ltd. (Wuhan, China). Capture hairpin DNA (H1), probe hairpin DNA (H2), HIV-DNA, 1-base mismatch DNA, 3-base mismatch DNA, hepatitis B virus DNA (HBV), and hepatitis C virus DNA (HCV) were purified with HPLC and obtained from Sangon Biotech. The details are shown in Table S1 in the Supporting Information (SI). Fetal bovine serum (FBS) was obtained from Gibco.

MPI-E electroluminescence workstation and CHI 660E electrochemical workstation were used to collect ECL and electrochemical date, respectively. Dynamic light scattering (DLS, Malvern), UV-2550 (Shimadzu, Japan), and trans-

DOI: 10.1021/acs.analchem.9b01969
Anal. Chem. 2019, 91, 12238−12245

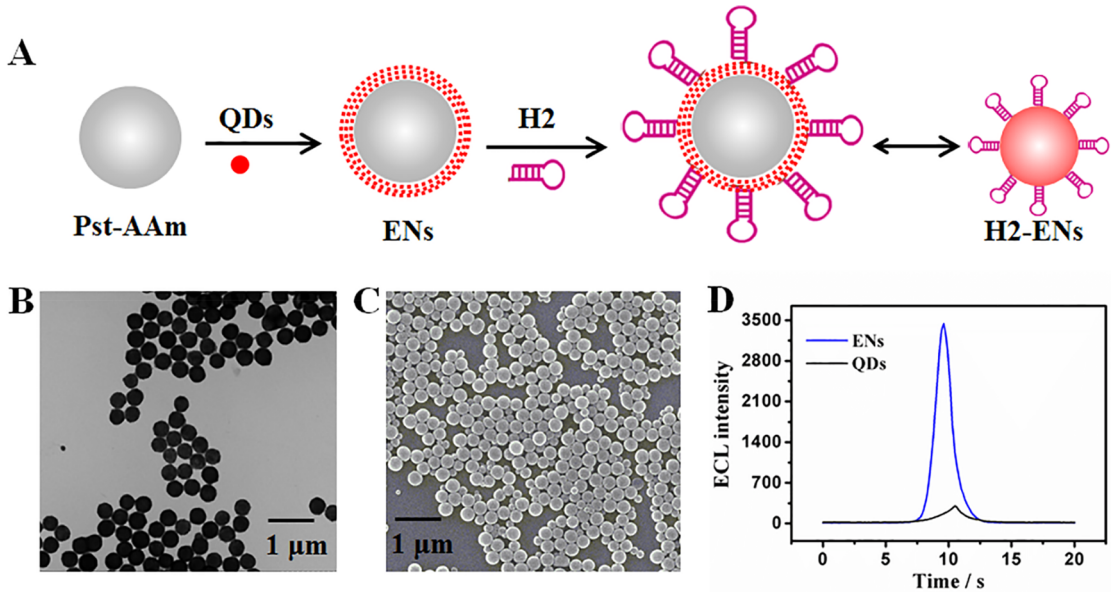

Figure 1. (A) Schematic diagram of preparation and modification of ENs. TEM image (B) and SEM image (C) of ENs. (D) ECL spectra under the same concentration of ENs and QDs.

mission electron microscopy (TEM, FEI Tecnai G2 20 TWIN) were used to characterize the size, dispersity, and surface potential of nanomaterials.

Preparation and Modification of ENs. Uniform poly(styrene/acrylamide) nanospheres (Pst-AAm) with several hundred nanometers were prepared based on the reported method.[32,38] The ENs were prepared by assembling three layers of CdSe/ZnS QDs on Pst-AAm surface. First, 200 μL 0.01 M pH 7.2 PBS containing 75 g/L NHS and 200 μL PBS containing 125 g/L EDC were added into 2 mL Pst-AAm. After mixing, 1 mL 0.2 g/mL polyethylenimine (PEI) was added and incubated for 10 h with shaking. Then the solution was centrifuged, and the precipitation was washed with NaCl, ultrapure water, and ethanol, respectively. The precipitation was redistributed into 1.6 mL hexyl alcohol containing a certain amount of CdSe/ZnS QDs and reacted for 2 h. After centrifuging and washing with *n*-hexane, ethanol, and ultrapure water, 1.6 mL PBS containing 0.01 g/mL PEI was added and reacted for 2 h. Three layers of QDs were layer-by-layer assembled onto Pst-AAm surface by repeating the assembly process of PEI and QDs. Carboxyl-functioned ENs was further prepared by silanization and succinic anhydride reaction for coupling with H2, the detail was shown in the SI.

To modify H2 on the surface of ENs, 100 μL ENs was added to 200 μL PBS containing 50 mM EDC and NHS for 30 min with shaking. After centrifuging and washing with PBS, 200 μL PBS containing 50 μM H2 was added and reacted at 37 °C for 2 h. Then the complexes were centrifuged and washed with PBS three times to obtain H2 modified ENs (H2-ENs). Finally, the H2-ENs were blocked with 1% BSA and placed at 4 °C for subsequent use.

Detection of HIV-DNA with the Multiple Amplified ECL Biosensor. First, H1 modified MBs (H1-MBs) were prepared. MBs (50 μL) were mixed with 200 μL 0.01 M pH 6.1 PBS containing 50 mM EDC and NHS. After being activated for 30 min with gentle shaking and washing with 0.01 M pH 7.2 PBS, 200 μL PBS with 50 μM H1 was added and further incubated at 37 °C for 2 h to obtain H1-MBs. After washing with PBS and blocking with 1% BSA, the H1-MBs were stored at 4 °C.

The HIV-DNA detection was based on the integration of MBs, ENs with SDA. First, each 10 μL H1-MBs was added into the samples containing different concentrations of HIV-DNA and reacted for 1 h to obtain H1-MBs/HIV-DNA complexes. After magnetic separation on a magnetic scaffold and washing with PBS, each 200 μL PBS with 10 μL H2-ENs was added and further incubated at 37 °C for 45 min to obtain H1-MBs/HIV-DNA/H2-ENs complexes. The addition of H2 could initiate SDA resulted from the more abundant binding sites between H2 and H1. Finally, the magnetic complexes were captured by a M-GCE and ECL signals were obtained in 2 mL PBS (0.1 M pH 7.2) containing 0.1 M $K_2S_2O_8$ based on a cyclic voltammetry (CV) scanning from 0 V to −1.65 V. The scan rate and the voltage of photomultiplier tube were 0.15 V/s and 900 V, respectively. Ag/AgCl and Pt wire were used as reference and counter electrode, respectively.

In order to investigate the amplification effect of SDA, two nucleic acid sequences (S1:5′-NH_2-$(CH_2)_6$-ATG TGG AAA AT-3′; S2:5′-CTC TAG CAG T-$(CH_2)_6$-NH_2-3′) were designed. Then S1-modified MBs and S2-modified ENs were fabricated based on the above modification process. After reacting with different concentrations of HIV-DNA, the ECL signals in 2 mL 0.1 M pH 7.2 PBS containing 0.1 M $K_2S_2O_8$ were recorded to compare with the signals obtained by SDA.

Specific Detection of HIV-DNA in Complex Samples. First, 0.15 nM HIV-DNA was mixed with 100 μL of milk, urine, FBS, and whole blood, respectively. Then each 10 μL H1-MBs was added to hybridize with target HIV-DNA. After reaction at for 1 h and magnetic separation on a magnet scaffold, each 10 μL H2-ENs was added to conduct SDA reaction and obtained magnetic H1-MBs/HIV-DNA/H2-ENs complexes. Four control experiments in the complex samples were conducted under the same conditions except no HIV-DNA was added. The ECL signals in 0.1 M $K_2S_2O_8$ were recorded.

DOI: 10.1021/acs.analchem.9b01969
Anal. Chem. 2019, 91, 12238−12245

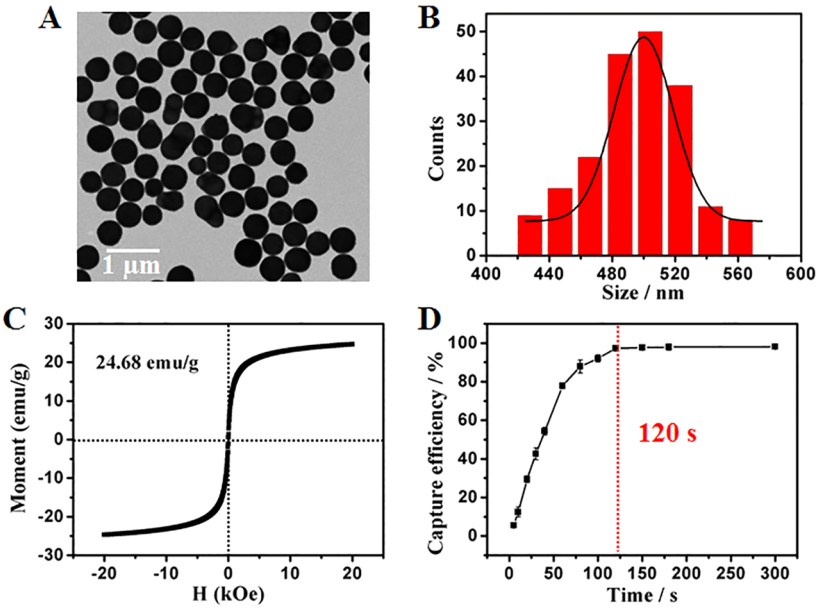

Figure 2. TEM image (A), diameter distribution (B), hysteresis loop (C), and magnetic response time curve (D) of MBs.

RESULTS AND DISCUSSION

ENs-Amplified ECL Detection. On the basis of assembly method, a novel kind of ECL emitter ENs was prepared by assembling three layers of CdSe/ZnS QDs onto Pst-AAm surface. H2 was further modified onto ENs surface through amide bond after the activation of EDC and NHS (Figure 1A). TEM and SEM images were applied to characterize the size and morphology of ENs. The prepared ENs exhibited good uniformity and dispersion with an average diameter of 330 nm (Figure 1B,C). An obvious fluorescence emission peak of ENs at 608 nm was observed under the excitation of 380 nm (Figure S1A, SI). And the ENs turned into bright red balls under a fluorescence inverted microscope (Figure S1B, SI). The above results showed that the prepared ENs retained the optical properties of QDs well. In addition to fluorescence signals, the ENs were found to have strong ECL signals with the help of coreactant $K_2S_2O_8$ (Figure S1C, SI), possessing high signal-to-background ratio for sensitive analysis. ECL that combines electrochemistry and chemiluminescence has emerged to be a powerful analytical method resulted from its fast response, high signal-to-noise ratio and cost-effective.[16] Compared to QDs, the same concentration of ENs could amplify the ECL signal by about 11.3-fold (Figure 1D). Thus, the prepared ENs not only had strong ECL signal by increasing the stowage of QDs on each nanosphere surface, but also solved the problem of low luminescence quantum efficiency of QDs. In theory, the more layers of QDs, the stronger ECL signal becomes. However, more layers of QDs will increase the complexity in preparation of ENs and the size of nanospheres.[35] Therefore, three layers of QDs were selected to prepare ENs, which exhibited a strong ECL signal and appropriate size.

Taking advantage of the large specific surface area and rich carboxyl groups of ENs, H2 was modified on the ENs surface to fabricate signal probes. After reacting with H2, the zeta potential of ENs changed from −31.4 mV to −25.3 mV, demonstrating the successful preparation of H2-ENs (Figure S2A, SI). The comparable ECL signals between H2-ENs and ENs (Figure S2B, SI) demonstrated the negligible effect of H2 modification on ECL signals. To further estimate the number of H2 on each EN, the curve between EN concentrations and its fluorescence intensity at 608 nm and the relationship between H2 concentrations and UV−vis absorption intensity at 260 nm were obtained (Figure S2C,D, SI). Then the concentrations of ENs and H2 in the sample could be calculated from the above two linear equations.[34] The number of H2 on each EN was calculated to be about 4.2×10^3, offering abundant binding sites and the feasibility of H2-ENs as signal probes in ECL biosensors.

In short, a new kind of EN was prepared with good uniformity, dispersity, and strong ECL signals, providing the feasibility for sensitive ECL detection.

MBs-Enabled Efficient Capture and Separation of HIV-DNA. In clinical diagnosis, the detection of HIV-DNA usually meets the problem of signal accuracy where coexisting components have significant interference on the experiment results.[26] False positive or negative signals will affect the accuracy of detection. Considering its unique separation and enrichment ability, MBs were used to separate HIV-DNA from complex matrix. From the TEM image, the MBs have homogeneous size, good dispersion, and water solubility (Figure 2A). The average diameter of MBs was calculated to be 494 ± 5.6 nm by randomly counting 200 nanospheres (Figure 2B). It can be seen from the hysteresis loop (Figure 2C) that the MBs had superparamagnetism and the saturation magnetization was 24.68 emu/g. Therefore, MBs could be gathered together under the external magnet and also be quickly dispersed into the solution after the magnet was removed.[35,36] The capture efficiency of MBs was close to 100% in 120 s on a magnetic scaffold (Figure 2D), indicating the strong magnetic response ability of MBs and 120 s was selected as the adsorption time of MBs during washing processes. On the basis of the amide bond reaction, H1 was modified to the surface of MBs to fabricate capture probes, and DLS was applied to characterize the modification process (Figure S3A, SI). The number of H1 on each MB was estimated to be about 1.4×10^3, and the details are shown in Figure S3B,C in the SI. With so many binding sites, H1-MBs could efficiently capture and separate HIV-DNA from complex samples.

DOI: 10.1021/acs.analchem.9b01969
Anal. Chem. 2019, 91, 12238−12245

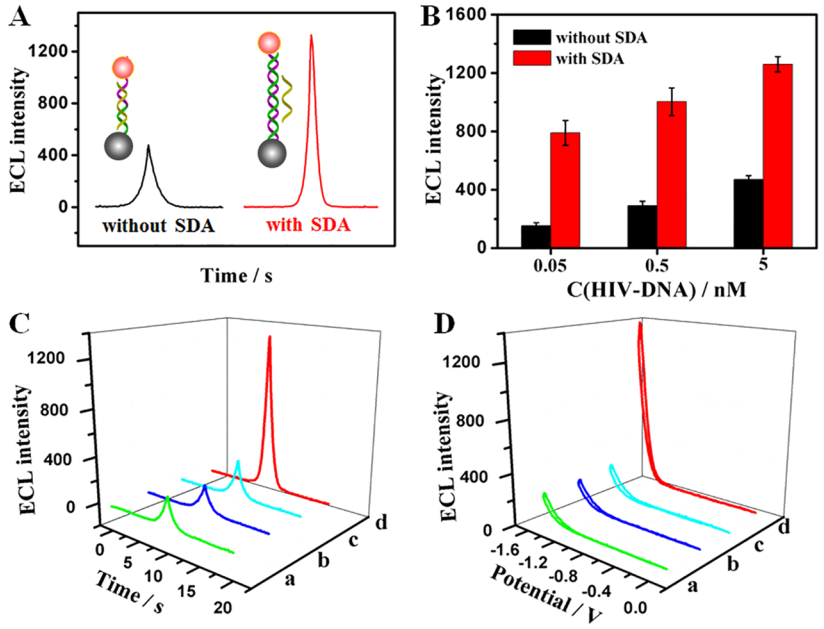

Figure 3. (A) ECL spectra of simple base complementary pairing hybridization (without SDA) and strand displacement amplification (with SDA). (B) ECL intensities with or without SDA under different HIV-DNA concentrations. (C) ECL-time curves under different detection conditions: (a) without H1, (b) without H2, (c) without HIV-DNA, and (d) all exist. (D) ECL-potential curves corresponding to (a–d).

The prepared H1-MBs could easily capture and separate targets with the help of a magnetic scaffold, facilitating the application of ECL in complex biological systems. However, how to transfer the magnetic complexes from the solution to the surface of working electrodes for signal collection is also a major problem to be considered. Herein, M-GCE with flexible magnetic response ability was used as working electrodes to capture magnetic complexes (Figure S4A, SI). The number of magnets in the M-GCE was optimized to decrease its influence on ECL signals. Compared to GCE, the ECL signal of M-GCE with four pieces of magnet was significantly decreased (Figure S4B, SI), indicating that the magnet had an effect on the ECL signals of ENs. The possible reason was the strong absorbance of magnets in the UV–vis region, which might attenuate ECL signals.[38] However, when the number of magnets was reduced to one piece, the ECL signal of M-GCE was comparable with GCE and the signal-to-background ratio was big enough for sensitive analysis (Figure S4C, SI). The magnetic response ability of M-GCE was strong enough to realize efficient enrichment and separation of the magnetic complexes from solution. Therefore, the M-GCE with one piece of magnet was chosen as working electrodes in the experiment.

Amplification Efficiency of SDA. In order to improve the sensitivity of the analysis method, the number of target molecules can be increased in addition to enhancing the load of signal molecules to amplify the signal. Especially for nucleic acid detection, many target amplification strategies have been established, including rolling circle amplification, SDA, and isothermal amplification, etc.[39] Among them, SDA needs neither continuous heating/cooling process nor external biological enzyme catalysis, with mild reaction conditions and high amplification efficiency. Herein, the addition of H2-ENs could initiate SDA reaction since H2 has more binding sites with H1 and then HIV-DNA would release into the solution for cycle amplification. The feasibility of SDA was characterized by polyacrylamide gel electrophoresis, and the details are shown in Figure S5A of the SI. In order to investigate the amplification efficiency of SDA, a control experiment without SDA was designed by using S1 and S2. S1 and S2 were the DNA oligonucleotides capable of simple base complementary pairing hybridization with target DNA. On the basis of the amide bond reaction, S1 and S2 were modified on the carboxyl-rich surface of MBs and ENs to prepare S1-MBs and S2-ENs, respectively. In the presence of target DNA, each target DNA combined at most a single EN. The introduction of SDA could increase the number of target DNA and ENs. After the SDA reaction, one H1-MBs was combined with more than one H2-ENs (Figure S5B, SI), greatly enhancing the ECL signals. In the presence of 5 nM HIV-DNA, the ECL signal of SDA was obviously higher than that of the control group (Figure 3A). To further explore this phenomenon, the ECL intensities of three parallel experiments under different HIV-DNA concentrations (0.05, 0.5, 5 nM) were recorded. As shown in Figure 3B, SDA could improve ECL signals by about 3.77-fold, further improving the detection sensitivity.

Therefore, H1-MBs, H2-ENs, and SDA were combined to fabricate a multiple amplified ECL biosensor for HIV-DNA detection. Four control experiments were designed to investigate the feasibility of the biosensor, including without H1, without H2, without HIV-DNA and all exist, respectively. As shown in Figure 3C,D, the ECL signal of (d) was obviously higher than that of the other three groups. The possible reasons were as follows: (1) The MBs neither captured targets nor reacted with H2-ENs without H1 modification. After magnetic separation, only MBs on M-GCE surface had no ECL signal. (2) In the absence of H2, H1-MBs could achieve targets capture and separation, but could not directly react with ENs. After magnetic separation, the H1-MBs/HIV-DNA also could not generate ECL signals. (3) H1-MBs did not react with H2-ENs in the absence of targets, so the ECL signal was also negligible.[23] (4) Only in the presence of all reagents, H1-MBs/HIV-DNA/H2-ENs complexes were successfully formed onto M-GCE surface, and a strong ECL signal could be obtained.

DOI: 10.1021/acs.analchem.9b01969
Anal. Chem. 2019, 91, 12238–12245

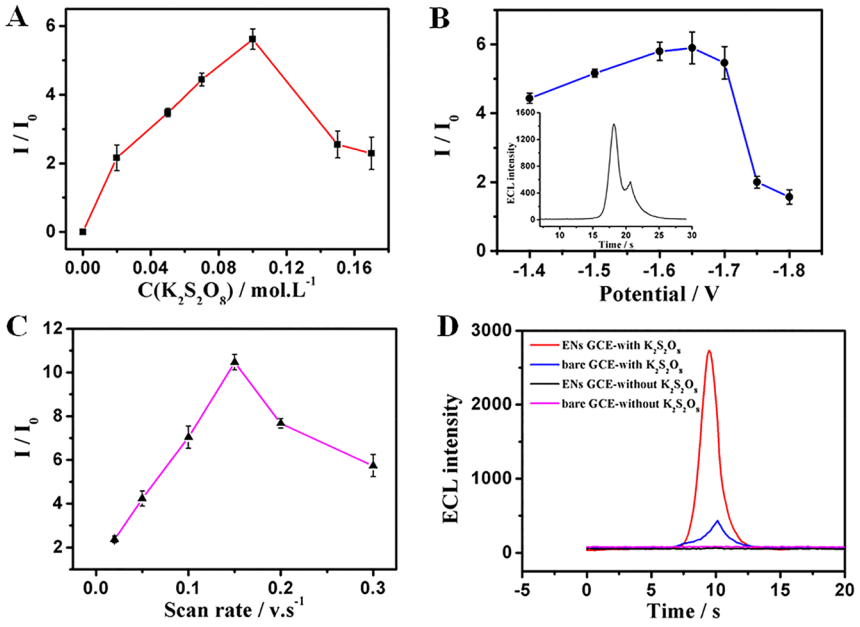

Figure 4. Optimization of detection conditions (I: ECL intensity; I_0: background): (A) $K_2S_2O_8$ (0, 0.02, 0.05, 0.07, 0.1, 0.15, 0.17 M), (B) negative potential (−1.4, −1.5, −1.6, −1.65, −1.7, −1.75, and −1.8 V), and (C) scan rate (0.02, 0.05, 0.1, 0.15, 0.2, and 0.3 V/s). (D) ECL spectra under different conditions.

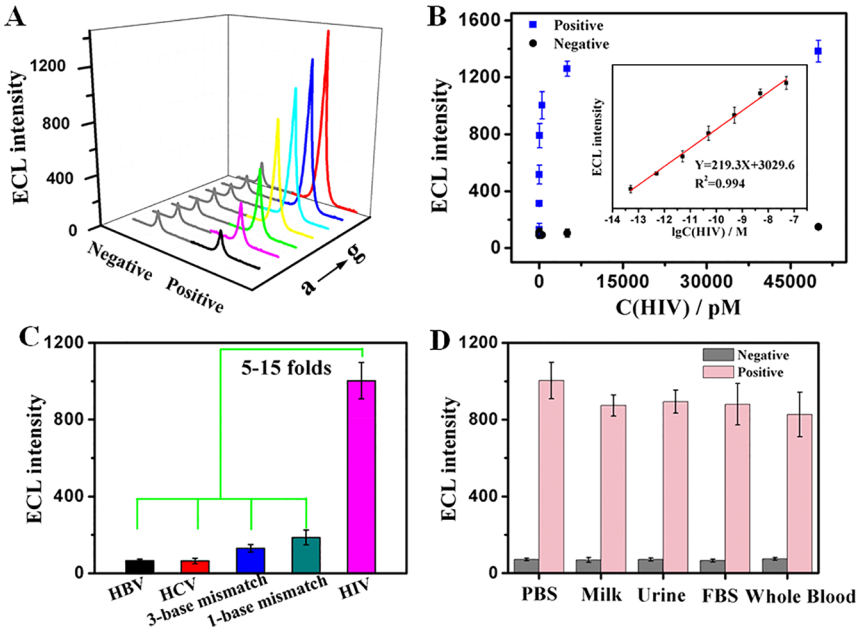

Figure 5. (A) ECL spectra of negative experiments (without HIV-DNA) and positive experiments under different HIV-DNA concentrations (a−g: 0.05 pM, 0.5 pM, 5 pM, 50 pM, 0.5 nM, 5 nM, and 50 nM). (B) Corresponding relationship between ECL intensities and HIV-DNA concentrations (Inset: linear curve). (C) Specificity of HIV-DNA detection. (D) Detection of HIV-DNA in complex samples.

The above results showed that SDA could further enhance detection sensitivity and the integration of MBs, ENs, and SDA ensured the good specificity and accuracy of the ECL biosensor for HIV-DNA detection.

Optimization of Detection Conditions. The luminescence principle of ECL includes annihilation and coreactant type, and the ECL signal of ENs belongs to the latter.[19,40] Therefore, the concentration of coreactant $K_2S_2O_8$ may affect the ECL signal of ENs. The ECL and background signals of ENs at different $K_2S_2O_8$ concentrations were recorded. As shown in Figure 4A, the signal-to-background ratio increased with the concentration until it reached the maximum at 0.1 M. Sufficient $K_2S_2O_8$ can ensure complete reaction with ENs, but too high concentration of coreactant might produce strong background interference.

Furthermore, the curve between signal-to-background ratio and negative potentials was obtained under the condition of $K_2S_2O_8$ concentration of 0.1 M (Figure 4B). At the beginning, the ratio changed little, and it decreased sharply after −1.65 V. Appropriate negative potential is beneficial for the reduction of QDs and coreactant as well as the electron transfer between ENs and the electrode surface. However, the single peak of

DOI: 10.1021/acs.analchem.9b01969
Anal. Chem. 2019, 91, 12238−12245

ECL spectrum changed to be a double peak after −1.65 V (Figure 4B, Inset) and the ratio decreased, which might result from the creation of a new electron−hole recombination.[41]

The effect of scan rate on ENs was also investigated by recording the signal-to-background ratio at different scan rates (Figure 4C). The ratio increased with the scan rate and tended to the maximum at 0.15 V/s. The faster the scan rate, the easier it is for electroactive substances to diffuse to the electrode surface. However, the active substances near electrode surface have no time to react if the scan rate is too fast. An optimal ratio of 10.3 could be obtained when the concentration of $K_2S_2O_8$, the negative potential, and the scan rate were 0.1 M, − 1.65 V, and 0.15 V/s, respectively.

Under optimized conditions, four control experiments were designed to explore the ECL specificity of ENs. The ECL signals were negligible in the absence of $K_2S_2O_8$ (Figure 4D). When there was no ENs, the presence of $K_2S_2O_8$ produced a weak signal. Only in the presence of $K_2S_2O_8$ and ENs simultaneously, an obvious ECL signal appeared, which not only proved that the ECL signals of ENs belonged to a coreactant type, but also indicated the good specificity of ENs as signal labels.

Sensitive ECL Detection of HIV-DNA. Using MBs as capture carriers, assembled ENs as signal labels, and SDA for signal enhancement, an "enrichment−stowage−cycle" strategy was proposed to fabricate a multiple amplified ECL biosensor for HIV-DNA detection. The ECL intensities increased with the concentrations of HIV-DNA and a good linear curve between ECL signals and the logarithm of HIV-DNA concentrations appeared from 0.05 pM to 50 nM (Figure 5A,B). The method not only had a wide dynamic range spanning 6 orders of magnitude, but also had a low detection limit of 39.81 fM, which was more sensitive than other reported HIV-DNA detection methods (Table S2, SI).[7,9,23,42,43] The higher sensitivity and wider dynamic range was attributed the following: (1) Due to its superparamagnetism, strong magnetic response, and large specific surface area, MBs could not only increase the load of H1 molecules, but also achieve efficient enrichment and separation of HIV-DNA from complex samples;[30] (2) Multiple QDs could be assembled on the surface of each nanosphere, and the prepared ENs could enhance the ECL signals by about 11.3-fold, effectively improving the detection sensitivity as signal labels; (3) The integration of SDA could realize cyclic amplification of the targets and further improved the ECL signals by about 3.77-fold, which was beneficial for low-abundant target detection. The same electrode was repeatedly scanned seven times during signal acquisition (Figure S6, SI). The comparability of ECL signals with each other indicated the stability of the method. The little decrease might result from the consumption of electroactive substances near electrode surface.

Furthermore, intra-assay and interassay variability were obtained to investigate the reproducibility of the method (Table 1). The intra-assay variability was calculated by parallel detection of three different concentrations of HIV-DNA by the same batch of H2-ENs, while the interassay variability was calculated by different batches of H2-ENs. The intra-assay and interassay variability were estimated to be 7.7% and 8.0%, respectively, indicating the good reproducibility of the method. The main reason was the uniform size, good stability, and dispersion of the ENs and MBs.

In practical applications, the detection method is needed to determine the symptom with high accuracy to realize timely treatment. To investigate the specificity of the method for HIV-DNA detection, four control groups were designed, including 20 nM HBV, 50 nM HCV, 10 nM 3-base mismatch DNA, and 5 nM 1-base mismatch DNA. Although the concentration of the control group was 10−100 times higher than that of HIV-DNA, the ECL intensity of 0.5 nM HIV-DNA was 5−15-fold stronger than that of the control groups (Figure 5C). Even 1-base mismatch DNA could be discriminated from target HIV-DNA. The negligible ECL signals of the control groups demonstrated the wonderful specificity of the method.

Table 1. Reproducibility of the Multiple Amplified ECL Biosensor for HIV-DNA Detection

	intra-assay			interassay		
HIV-DNA	mean	SD	RSD (%)	mean	SD	RSD (%)
0.5 pM	313	15.3	4.9	356	15.2	4.3
50 pM	790	85.4	10.8	810	90	11.1
5 nM	1260	92.9	7.4	1217	104.1	8.6
	intra-assay variability 7.7%			interassay variability 8.0%		

In addition to the influence of analogues, the interference of matrix in complex samples may also affect the accuracy of the experimental results. Herein, 0.15 nM HIV-DNA was added into milk, urine, FBS, and whole blood, respectively, to prepare complex samples. Corresponding control groups were prepared using the same operation without HIV-DNA adding. After magnetic separation by H1-MBs, SDA reaction with H2-ENs and capture onto the surface of M-GCE, ECL signals of the experimental and control groups were recorded. The ECL signals of complex samples had good comparable signal-to-background ratios with PBS buffer (Figure 5D). The recovery rate of the method in complex samples was calculated to be 90.47∼105.7% (Table S3, SI), indicating the feasibility and accuracy of the method in practical applications. The above results indicated the excellent anti-interference capability of the method, which was mainly due to the stability and high capture efficiency of MBs in both buffer and complex samples.

In general, the multiple amplified ECL biosensor exhibited wonderful specificity, reproducibility, stability, anti-interference capability, and can be used for ultrasensitive HIV-DNA detection with wide dynamic range.

CONCLUSIONS

On the basis of the combination of MBs, ENs with SDA, an "enrichment−stowage−cycle" strategy was proposed to fabricate a multiple amplified ECL biosensor for HIV-DNA detection. H1-MBs could effectively capture and separate HIV-DNA from complex matrix directly, simplifying operation process and time. The prepared ENs by assembly method can enhance ECL signals by about 11.3-fold, solving the problem of low luminescent efficiency of QDs and achieving high signal-to-background ratio for sensitive analysis. Taking advantage of the further amplification of SDA, the fabricated ECL biosensor successfully realized HIV-DNA detection with high sensitivity, accuracy, specificity, and stability. The successful detection of HIV-DNA in complex samples (milk, urine, FBS, and whole blood) indicated its potential application in timely diagnosis of disease and measurement of low-abundant biomarkers in real samples.

DOI: 10.1021/acs.analchem.9b01969
Anal. Chem. 2019, 91, 12238−12245

■ ASSOCIATED CONTENT

Supporting Information

The Supporting Information is available free of charge on the ACS Publications website at DOI: 10.1021/acs.analchem.9b01969.

Sequences of oligonucleotides used in this assay (Table S1), optical properties of ENs (Figure S1), preparation and verification of H2-ENs (Figure S2), characterization of H1-MBs (Figure S3), optimization of M-GCE (Figure S4), amplification of SDA (Figure S5), summary of the detection of HIV-DNA with different methods (Table S2), stability of ECL signals (Figure S6), and recovery rate of the method in complex samples (Table S3) (PDF)

■ AUTHOR INFORMATION

Corresponding Authors

*E-mail: wenwei@hubu.edu.cn (W.W.).
*E-mail: wangsf@hubu.edu.cn (S.W.).

ORCID

Wei Wen: 0000-0001-6138-7470
Xiuhua Zhang: 0000-0003-3586-9921
Shengfu Wang: 0000-0001-7175-4908

Notes

The authors declare no competing financial interest.

■ ACKNOWLEDGMENTS

Z.W. and F.L. contributed equally to this work. This work was supported by the National Natural Science Foundation of China (21405035, 21475032, 21775033) and the General Project Program of the Natural Science Foundation of Hubei Province (2017CFB529).

■ REFERENCES

(1) Zou, L.; Ling, L. *Anal. Chem.* **2018**, *90*, 13373−13377.
(2) WHO Website. HIV/AIDS. Updated December 2017. https://www.who.int/gho/hiv/en/.
(3) Moore, J. *AIDS* **1990**, *4*, 297−306.
(4) Isola, N. R.; Stokes, D. L.; Vo-Dinh, T. *Anal. Chem.* **1998**, *70*, 1352−1356.
(5) Driver, G. A.; Patton, J. C.; Moloi, J.; Stevens, W. S.; Sherman, G. G. *J. Virol. Methods* **2007**, *146*, 397−400.
(6) Wang, Y.; Bai, X.; Wen, W.; Zhang, X.; Wang, S. *ACS Appl. Mater. Interfaces* **2015**, *7*, 18872−18879.
(7) Long, Y.; Zhou, C.; Wang, C.; Cai, H.; Yin, C.; Yang, Q.; Xiao, D. *Sci. Rep.* **2016**, *6*, 23949.
(8) Sun, A. L.; Deng, K.; Fu, W. L. *Biosens. Bioelectron.* **2015**, *74*, 66−70.
(9) Gao, X.; Wang, X.; Li, Y.; He, J.; Yu, H. Z. *Anal. Chem.* **2018**, *90*, 8147−8153.
(10) Ye, Y. D.; Xia, L.; Xu, D. D.; Xing, X. J.; Pang, D. W.; Tang, H. W. *Biosens. Bioelectron.* **2016**, *85*, 837−843.
(11) Qaddare, S. H.; Salimi, A. *Biosens. Bioelectron.* **2017**, *89*, 773−780.
(12) Spadavecchia, J.; Barras, A.; Lyskawa, J.; Woisel, P.; Laure, W.; Pradier, C. M.; Boukherroub, R.; Szunerits, S. *Anal. Chem.* **2013**, *85*, 3288−3296.
(13) Lei, Y. M.; Xiao, B. Q.; Liang, W. B.; Chai, Y. Q.; Yuan, R.; Zhuo, Y. *Biosens. Bioelectron.* **2018**, *109*, 109−115.
(14) Chen, M. M.; Wang, Y.; Cheng, S. B.; Wen, W.; Zhang, X.; Wang, S.; Huang, W. H. *Anal. Chem.* **2018**, *90*, 5075−5081.
(15) Jiang, X.; Wang, H.; Wang, H.; Yuan, R.; Chai, Y. *Anal. Chem.* **2016**, *88*, 9243−9250.
(16) Li, L.; Chen, Y.; Zhu, J. J. *Anal. Chem.* **2017**, *89*, 358−371.
(17) Ding, Z.; Quinn, B. M.; Haram, S. K.; Pell, L. E.; Korgel, B. A.; Bard, A. J. *Science* **2002**, *296*, 1293−1297.
(18) Dong, Y. P.; Chen, G.; Zhou, Y.; Zhu, J. J. *Anal. Chem.* **2016**, *88*, 1922−1929.
(19) Wu, Z.; Hu, J.; Zeng, T.; Zhang, Z. L.; Chen, J.; Wong, G.; Qiu, X.; Liu, W.; Gao, G. F.; Bi, Y.; Pang, D. W. *Anal. Chem.* **2017**, *89*, 2039−2048.
(20) Tian, C. Y.; Xu, J. J.; Chen, H. Y. *Chem. Commun.* **2012**, *48*, 8234−8236.
(21) Wang, X. F.; Zhou, Y.; Xu, J. J.; Chen, H. Y. *Adv. Funct. Mater.* **2009**, *19*, 1444−1450.
(22) Bao, T.; Wen, W.; Zhang, X.; Xia, Q.; Wang, S. *Biosens. Bioelectron.* **2015**, *70*, 318−323.
(23) Deng, X.; Wang, C.; Gao, Y.; Li, J.; Wen, W.; Zhang, X.; Wang, S. *Biosens. Bioelectron.* **2018**, *105*, 211−217.
(24) Wang, D.; Li, Y.; Lin, Z.; Qiu, B.; Guo, L. *Anal. Chem.* **2015**, *87*, 5966−5972.
(25) Shao, K.; Wang, J.; Jiang, X.; Shao, F.; Li, T.; Ye, S.; Chen, L.; Han, H. *Anal. Chem.* **2014**, *86*, 5749−5757.
(26) Fang, H.; Xie, N.; Ou, M.; Huang, J.; Li, W.; Wang, Q.; Liu, J.; Yang, X.; Wang, K. *Anal. Chem.* **2018**, *90*, 7164−7170.
(27) Wu, Z.; Guo, W. J.; Bai, Y. Y.; Zhang, L.; Hu, J.; Pang, D. W.; Zhang, Z. L. *Anal. Chem.* **2018**, *90*, 1683−1690.
(28) Wang, Y.; Gan, N.; Zhou, Y.; Li, T.; Hu, F.; Cao, Y.; Chen, Y. *Biosens. Bioelectron.* **2017**, *97*, 100−106.
(29) Rodriguez, N. M.; Wong, W. S.; Liu, L.; Dewar, R.; Klapperich, C. M. *Lab Chip* **2016**, *16*, 753−763.
(30) Wu, Z.; Zhou, C. H.; Chen, J. J.; Xiong, C.; Chen, Z.; Pang, D. W.; Zhang, Z. L. *Biosens. Bioelectron.* **2015**, *68*, 586−592.
(31) Chikkaveeraiah, B. V.; Bhirde, A.; Morgan, N. Y.; Eden, H. S.; Chen, X. *ACS Nano* **2012**, *6*, 6546−6561.
(32) Wen, C. Y.; Wu, L. L.; Zhang, Z. L.; Liu, Y. L.; Wei, S. Z.; Hu, J.; Tang, M.; Sun, E. Z.; Gong, Y. P.; Yu, J.; Pang, D. W. *ACS Nano* **2014**, *8*, 941−949.
(33) Yang, J.; Lim, E. K.; Lee, H. J.; Park, J.; Lee, S. C.; Lee, K.; Yoon, H. G.; Suh, J. S.; Huh, Y. M.; Haam, S. *Biomaterials* **2008**, *29*, 2548−2555.
(34) Wu, Z.; Zeng, T.; Guo, W. J.; Bai, Y. Y.; Pang, D. W.; Zhang, Z. L. *ACS Appl. Mater. Interfaces* **2019**, *11*, 5762−5770.
(35) Hu, J.; Jiang, Y. Z.; Tang, M.; Wu, L. L.; Xie, H.; Zhang, Z. L.; Pang, D. W. *Anal. Chem.* **2019**, *91*, 1178−1184.
(36) Hong, S. L.; Zhang, Y. N.; Liu, Y. H.; Tang, M.; Pang, D. W.; Wong, G.; Chen, J.; Qiu, X.; Gao, G. F.; Liu, W.; Bi, Y.; Zhang, Z. L. *Anal. Chem.* **2018**, *90*, 7310−7317.
(37) Huang, Z. J.; Han, W. D.; Wu, Y. H.; Hu, X. G.; Yuan, Y. N.; Chen, W.; Peng, H. P.; Liu, A. L.; Lin, X. H. *J. Electroanal. Chem.* **2017**, *785*, 8−13.
(38) Xie, M.; Hu, J.; Wen, C. Y.; Zhang, Z. L.; Xie, H. Y.; Pang, D. W. *Nanotechnology* **2012**, *23*, 035602.
(39) Zhao, Y.; Chen, F.; Li, Q.; Wang, L.; Fan, C. *Chem. Rev.* **2015**, *115*, 12491−12545.
(40) Liu, S.; Zhang, X.; Yu, Y.; Zou, G. *Anal. Chem.* **2014**, *86*, 2784−2788.
(41) Liu, S.; Zhang, Q.; Zhang, L.; Gu, L.; Zou, G.; Bao, J.; Dai, Z. *J. Am. Chem. Soc.* **2016**, *138*, 1154−1157.
(42) Wang, L.; Tian, J.; Yang, W.; Zhao, Y.; Zhao, S. *Luminescence* **2016**, *31*, 573−579.
(43) Yan, X.; Tang, M.; Yang, J.; Diao, W.; Ma, H.; Cheng, W.; Que, H.; Wang, T.; Yan, Y. *RSC Adv.* **2018**, *8*, 31710−31716.

DOI: 10.1021/acs.analchem.9b01969
Anal. Chem. 2019, 91, 12238−12245